Dimerization of a His117Gly Azurin Mutant by External Addition of 1,ω-Di(imidazol-1-yl)alkanes

Gertie van Pouderoyen, Tanneke den Blaauwen, Jan Reedijk, and Gerard W. Canters*

Leiden Institute of Chemistry, Gorlaeus Laboratories, Leiden University, Leiden, The Netherlands

Received April 17, 1996[⊗]

ABSTRACT: The possibility to construct non-covalently linked protein dimers was investigated by employing the His117Gly mutant of the Cu containing azurin and the bifunctional 1,ω-di(imidazol-1-yl)alkanes as linkers. The His117Gly mutation creates a gap in the coordination sphere of the metal through which the latter becomes accessible for externally added ligands. The bifunctional ligands gave rise to the formation of dimers provided the linker was sufficiently long, as in the case of 1,ω-di(imidazol-1-yl)pentane and -hexane; the butane linker only produced monomers. The binding of the azurin molecules to the bifunctional C_5 and C_6 linkers showed cooperativity, which is the result of the hydrophobic interaction of the aligned hydrophobic patches. The energy and surface area involved in this process have been estimated from the experimental data to be ΔG is −1.3 to −2.1 kcal/mol and 65−105 Å^2. The implications for the study of electron transfer processes inside a protein matrix are indicated.

In recent studies we have shown that it is possible to replace the ligands of a metal in the active site of a protein by external ligands. This was first demonstrated on the blue-copper protein, azurin from *Pseudomonas aeruginosa*, which functions as an electron carrier in a variety of bacterial respiratory chains, and which has a single copper ion in its active site. The Cu is held in place by three strong equatorial ligands, His46 and His117 which both coordinate with their Nδ-atoms, and Cys112 which coordinates the Cu by its Sγ-atom (see Figure 1). In addition there are two axially interacting groups, Met121 coordinating with its Sδ atom and Gly45 coordinating with its backbone carbonyl oxygen (see Figure 1).

Of these five residues only His117 protrudes through the protein surface. Replacing it by a glycine creates a hole through which the Cu becomes directly accessible from the outside for a large variety of ligands. For instance, addition of (substituted) imidazoles to the Cu(II) containing His117Gly azurin restores the original spectroscopic features of the wild-type (wt)[1] Cu-site (den Blaauwen et al., 1991, 1993; den Blaauwen & Canters, 1993). In a subsequent exploration also His46, which is buried inside the protein, was replaced by a glycine. The cavity created inside the protein in this way can again be filled by externally added ligands, leading to so-called type-1 or type-2 Cu-sites, which exhibit a variety of spectroscopic features (van Pouderoyen et al., 1996). When the axial methionine-121 is replaced by a glycine again the created hole is able to bind externally added ligands (Vidakovic & Germanas, 1995).

Partly inspired by this work other research groups expanded on the idea of making a gap in the coordination sphere of the metal in the active site of a metalloenzyme [for a review see Barrick (1995)]. Mutations have been applied to heme-containing proteins by which an axial histidine was replaced by an amino acid with a small side chain. This made it possible to bind externally added ligands inside the newly created hole (Barrick, 1994; McRee et al., 1994; Wilks et al., 1995). In a similar vein the replacement of an axially coordinating methionine by an alanine or an adjacent tryptophan by a glycine has been reported for heme-containing proteins (Lu et al., 1993; Fitzgerald et al., 1994). Also in these cases it appeared possible to fill the internal hole in the protein structure by externally added residues.

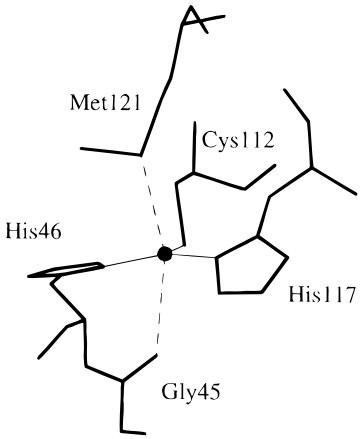

FIGURE 1: Schematic representation of the copper site of wt azurin.

We thought it worthwhile to investigate whether our original idea could be extended to the creation of dimers. An organic linker containing coordinating groups at opposite ends would be sufficient (in principle) to bind two mutated proteins. As the coordinating groups insert spontaneously into the gaps created by the mutations, an easy and gentle way would have been found to construct dimers, or chimera's of two protein domains. Moreover, a simple means would be available to connect the redox centres in two domains by a conducting bridge. Thus, the electron transfer across a bridge completely buried inside a protein matrix could be studied as a function of the bridge properties (saturated/

* Address correspondence to this author at Leiden Institute of Chemistry, Gorlaeus Laboratories, Leiden University, P.O. Box 9502, 2300 RA Leiden, The Netherlands. Tel: 31 71 527 4256. Fax: 31 71 527 4349. E-mail: Canters@Rulgca.LeidenUniv.nl.

[⊗] Abstract published in *Advance ACS Abstracts,* September 1, 1996.

[1] Abbreviations: 1,4-dib, 1,4-di(imidazol-1-yl)butane; 1,5-dip, 1,5-di(imidazol-1-yl)pentane; 1,6-dih, 1,6-di(imidazol-1-yl)hexane; *N*-meim, *N*-methylimidazole; wt, wild-type.

S0006-2960(96)00931-2 CCC: $12.00

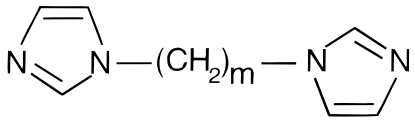

FIGURE 2: 1,ω-Di(imidazol-1-yl)alkanes used in this study (m = 4, 5, or 6).

unsaturated character, presence of side groups, presence of heteroatoms).

Here we report on the prototype of this experiment by which the His117Gly azurin is reacted with a linker molecule that contains two imidazole-groups separated by a $(CH_2)_m$-bridge [1,ω-di(imidazol-1-yl)alkanes, m = 4, 5, or 6, see Figure 2). Dimer formation was observed, indeed. As the newly created cavity in the His117Gly mutant is located in the hydrophobic patch of azurin, these patches will interact when dimers are formed and this should give rise to cooperative binding of the the second azurin molecule. This was found to be the case also. The cooperativity of the dimer formation could be quantified by studying the stepwise binding of azurin to the bisimidazole ligand. The results are described below.

EXPERIMENTAL PROCEDURES

Protein Isolation. His117Gly azurin was isolated from *Escherichia coli* JM101 transformed with plasmid pTB46 and purified as apo-protein as described earlier (den Blaauwen et al., 1991; den Blaauwen & Canters, 1993).

Exogenous Ligands. The ligands 1,4-di(imidazol-1-yl)-butane (1,4-dib), 1,5-di(imidazol-1-yl)pentane (1,5-dip), and 1,6-di(imidazol-1-yl)hexane (1,6-dih) (see Figure 2 for structural formulas) were synthesized by using 1,ω-dibromoalkanes according to the alkylation procedures first reported by Roe (1963) for the synthesis of alkyl and benzyl imidazoles. Reacting the dibromoalkanes with a solution of imidazole and sodium in liquid ammonia (activated by traces of iron(III) chloride), good yields were obtained (I. M. M. Schellekens, unpublished observations). The purity of the reaction products was confirmed by 1D proton NMR spectroscopy. *N*-Methylimidazole (*N*-meim) was purchased from Sigma.

Ligand Binding. A stoichiometric amount of $Cu(NO_3)_2$ was added to a 0.1 mM apo-His117Gly azurin solution in 20 mM Mes, pH 6.0. The absorption at 420 nm was monitored, and when no further increase was observed (after about 30 min) the exogenous ligand was added as a concentrated solution to the protein solution. When, again, no further increase in the absorption was observed, a UV/vis spectrum was recorded at 298 K on a Shimadzu UV-2101PC spectrophotometer.

Job's Method of Continuous Variation. Job's method (Jones, 1964) was used to determine n in the equation describing the complex formation between molecules A and B according to $A + nB \rightleftarrows AB_n$. The experiments were performed on solutions in which the sum of the number of moles of A and B present is constant and equal to M. When $(1-x)V$ mL of an M molar solution of A are mixed with xV mL of an M molar solution of B to give a final volume of V, the maximum of $[AB_n]$ occurs at x_m with

$$n = x_m/(1-x_m) \qquad (1)$$

Experimentally the maximum of $[AB_n]$ is found by determining the extremum of the function Y (eq 2), which is the difference between the measured absorption and that predicted upon the assumption of no complex formation:

$$Y = [A]\epsilon_A + [B]\epsilon_B + [AB_n]\epsilon_{AB_n} - M(1-x)\epsilon_A - Mx\epsilon_B \qquad (2)$$

in which ϵ_A, ϵ_B, and ϵ_{AB_n} are the molar extinction coefficients of A, B, and AB_n at λ_{max} (Table 1), respectively.

Table 1: Extinction Coefficients at the Maximum of Absorbance (λ_{max}) of His117Gly Azurin with Various Exogenous Ligands

ligand	λ_{max}, (nm)	$\epsilon_{b,\lambda max,}$[a] ($mM^{-1}$ cm^{-1})
N-meim	630	5.96
1,5-dip	638	5.90
1,6-dih	632	5.63

[a] The estimated errors amount to ± 0.1 mM^{-1} cm^{-1}; the quoted values are per mM of bound azurin.

In the experiments performed here molecule A was *N*-meim, 1,4-dib, 1,5-dip, or 1,6-dih and molecule B was His117Gly azurin. V was 1 mL, M was 50 μM, and x varied between 0 and 1 in steps of 0.1. Y will exhibit a maximum in this case because $\epsilon_{AB_n} > \epsilon_A + \epsilon_B$. Experiments were performed in 20 mM Mes, pH 6.0, for 1,5-dip and 1,6-dih and in 20 mM Hepes, pH 7.5, for *N*-meim and 1,4-dib. 1.2 equiv of $Cu(NO_3)_2$ was added to the apo-His117Gly azurin prior to the addition of the imidazole derivative, and the resulting solution was incubated for 1 h at 298 K to reach equilibrium.

Extinction Coefficients. In the absence of externally added ligands the His117Gly azurin is a green protein at pH 6.0 with absorbances around 420 and 628 nm. These absorbances are respectively 19% and 14% of the absorbance at 280 nm ($\epsilon_{280} = 9.8 \times 10^3$ M^{-1} cm^{-1}) (den Blaauwen & Canters, 1993). To determine the His117Gly azurin concentrations an extinction coefficient at 628 nm of 1.37×10^3 M^{-1} cm^{-1} was used.

To determine the extinction coefficients of the azurin ligand complexes, 1 mL samples in a 1 cm cuvette were prepared by mixing various concentrations of apo-His117Gly azurin with 1.2−1.5 equiv of $Cu(NO_3)_2$ and a fixed excess of ligand in 20 mM Mes, pH 6.0. After reaching a maximum (in about 1 h at 298 K) the absorbance at ~630 nm was measured. For *N*-meim, the concentration used was 64 μM and the protein concentrations varied from 6 to 224 μM. For 1,5-dip and 1,6-dih, the concentration was 32 μM and the protein concentration varied from 3 to 50 μM. The extinction coefficients were determined from a plot of the absorbance against the total azurin concentration.

Scatchard Plot and Hill Coefficient. To study the ligand binding in the case of the *N*-meim−His117Gly azurin complex the same data as used for the determination of the extinction coefficient were used. In the case of the 1,5-dip and 1,6-dih complexes dilute samples had to be used to promote partial dissociation of the ligand. To obtain sufficient optical density in that case, cells with a 10 cm path length had to be used. Samples were prepared by mixing 1−17 μM apo-His117Gly azurin with 1.2−1.5 equiv of $Cu(NO_3)_2$ and 2.5 μM of 1,5-dip or 1,6-dih in 20 mM Mes, pH 6.0. The maximum absorbance at 638 or 632 nm, respectively, was reached in 1−1.2 h at 298 K; the absorbance was then determined on a Varian DMS 200 UV/vis spectrophotometer. To analyze the absorbance data and obtain equilibrium constants the following theoretical analysis was applied.

The ligands 1,5-dip and 1,6-dih have two imidazole groups or two "sites" that can bind to a His117Gly azurin molecule. In a solution containing ligand and His117Gly azurin part of the sites will be occupied by an azurin molecule ("bound sites") and part will be unoccupied ("free sites"). The absorbance, A_m, at the peak maximum (λ_{max}), around 630 nm, is given by

$$A_m = d\{[\mathrm{Az}]_f\,\epsilon_f + [s_b]\epsilon_b\} \quad (3)$$

in which d is the optical path length, $[\mathrm{Az}]_f$ is the concentration of free His117Gly azurin, ϵ_f is the extinction coefficient of the His117Gly azurin (1.37 mM^{-1} cm^{-1}), $[s_b]$ is the concentration of bound sites, and ϵ_b is the extinction coeffient of a bound site. The concentration of bound sites can be calculated from eq 4 in which $[\mathrm{Az}]_t$ is the total concentration of His117Gly azurin:

$$[s_b] = \{A_m - \epsilon_f\, d[\mathrm{Az}]_t\}/\{d(\epsilon_b - \epsilon_f)\} \quad (4)$$

Equation 4 was obtained by substituting $[\mathrm{Az}]_t - [s_b]$ fot $[\mathrm{Az}]_f$ in eq 3.

When the partial saturation of the ligand is defined as $y = [s_b]/[L]_t$, $[L]_t$ being the total concentration of ligand, the relation between y, the number of binding sites (n), and the binding constant (K_b) is given by eqs 5a and 5b.

$$y/[\mathrm{Az}]_f = nK_b - yK_b \quad \text{or} \quad (5a)$$

$$y/n = K_b[\mathrm{Az}]_f/\{1 + K_b[\mathrm{Az}]_f\} \quad (5b)$$

with $K_b \equiv [s_b]/\{[s_f][\mathrm{Az}]_f\}$. This assumes that the n binding sites are independent and have identical binding characteristics.

In a Scatchard plot (Scatchard, 1949; Cantor & Schimmel, 1980), $y/[\mathrm{Az}]_f$ is plotted against y (see eq 5a). The slope of the plot gives the binding constant K_b and the intercept equals the number of binding sites n (see eq 5a).

However, if the sites exhibit positive cooperativity the Scatchard plot has a concave-down appearance (Cantor & Schimmel, 1980) and eq 5 is not applicable.

For a ligand, L, with two sites, the following equilibria obtain

$$\mathrm{L} + \mathrm{Az} \rightleftarrows \mathrm{LAz}, \quad \text{with} \quad (6a)$$

$$K_{b1} = [\mathrm{LAz}]/\{[\mathrm{L}][\mathrm{Az}]_f\}, \quad \text{and} \quad (6b)$$

$$\mathrm{LAz} + \mathrm{Az} \rightleftarrows \mathrm{LAz}_2, \quad \text{with} \quad (6c)$$

$$K_{b2} = [\mathrm{LAz}_2]/\{[\mathrm{LAz}][\mathrm{Az}]_f\}. \quad (6d)$$

In the case of "complete cooperativity" the LAz concentration is vanishingly small and the equilibrium equations can be simplified to (Palmer, 1991)

$$\mathrm{L} + 2\mathrm{Az} \rightleftarrows \mathrm{LAz}_2, \quad \text{in which case} \quad (6e)$$

$$K_b = [\mathrm{LAz}_2]/\{[\mathrm{L}][\mathrm{Az}]_f^2\}, \quad \text{and} \quad (6f)$$

$$y/n = K_b[\mathrm{Az}]_f^2/\{1 + K_b[\mathrm{Az}]_f^2\}. \quad (6g)$$

When the dimer formation is not completely cooperative the fractional saturation of the ligand is given by the semi-empirical equation (eq 7) (Hill, 1910; Cantor & Schimmel, 1980; Palmer, 1991)

$$y/n = K_b[\mathrm{Az}]_f\,\alpha/\{1 + K_b[\mathrm{Az}]_f\,\alpha\} \quad (7)$$

in which α is the Hill coefficient ($1 \leq \alpha \leq 2$).

EPR Spectroscopy. 2 mM samples for EPR spectroscopy were prepared by addition of a stoichiometric amount of $Cu(NO_3)_2$ to a 0.1 mM apo-His117Gly protein solution in 20 mM Mes, pH 6.0. This was followed, after incubation of 0.5 h at room temperature, by the addition of a 10-fold excess of ligand. The samples were concentrated in an Amicon ultrafiltration cell, 0.2 M NaCl in 20 mM Mes, pH 6.0, was added to remove any adventitiously bound copper and the solution was concentrated again. The NaCl was then removed by at least 1000-fold dilution by addition of 20 mM Mes, pH 6.0, and concentration in the Amicon cell. 40% glycerol was added to the concentrated samples, and the pH was determined. For the ligand 1,4-dib a slightly different procedure was followed, because the method described above did give EPR spectra of several species (spectra not shown) and it was not clear if this arose from adventitiously bound copper or from other forms. Therefore the sample was made with the following changes in the procedure: no external ligand was added during the Amicon steps, and 0.05 mM EDTA was used instead of 0.2 M NaCl. The spectra of the Cu−protein were recorded (data not shown) to check that no adventiously copper was bound and 10 mM 1,4-dib was added to this sample. Spectra were recorded with a JEOL JESRE2X spectrometer at X-band at 77 K and interfaced with an ES-PRIT330 data manipulation system. Parameters for recording EPR spectra were typically 12.5 mT/min sweep rate, 0.32 mT field modulation width, 9.099 GHz frequency and 4 mW microwave power. The magnetic field was calibrated with α,α'-diphenyl-β-picrylhydrazyl.

Computer simulations of EPR spectra were based on the spin Hamiltonian $H = \beta B\mathbf{g}S + S\mathbf{A}I$ with $S = {}^1/_2$ and $I = {}^3/_2$ [69.1% ^{63}Cu and 30.9% ^{65}Cu; $\mathbf{A}(^{65}\mathrm{Cu}/^{63}\mathrm{Cu}) = 1.071$]. The **g**- and **A**-tensors were assumed to be colinear and the hyperfine interaction was taken as a perturbation to the Zeeman interaction to second-order (Pake & Estle, 1973). The intensity was calculated as described by Aasa and Vänngård (1975).

RESULTS AND DISCUSSION

Ligand Binding. Addition of 0.5 equiv of *N*-meim or 1,4-dib to a His117Gly solution resulted in a dramatic increase of the absorption at around 630 nm, indicating binding of ligand (den Blaauwen & Canters, 1993). Addition of extra ligand (1−5 equiv in total) gave a further increase of absorption (Figure 3A and B). In a similar experiment with 1,5-dip and 1,6-dih the addition of 0.5 equiv of ligand causes an increase of the absorption around 630 nm that is roughly twice that obtained with *N*-meim or 1,4-dib. Hardly any further increase in absorption was observed after further addition (0.5−5 equiv) of ligand (Figure 3C and D). This qualitative observation suggests that in the case of 1,5-dip or 1,6-dih both sites on the ligand bind azurin and thus promote the formation of azurin dimers. The 1,4-dib ligand behaves very similar to *N*-meim. Apparently the $(CH_2)_4$-

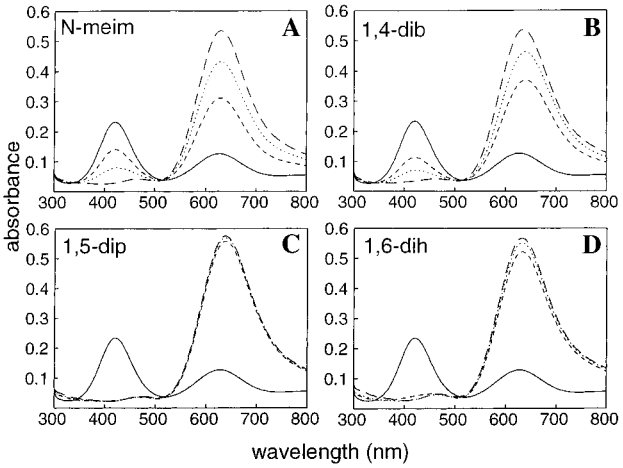

FIGURE 3: Room temperature UV/vis spectra of 0.1 mM His117Gly azurin samples with a stoichiometric amount of $Cu(NO_3)_2$ in 20 mM Mes buffer, pH 6 (solid line), and the spectra of the same samples after addition of 0.05 mM ligand (0.5 equiv; small dashes), 0.1 mM ligand (1.0 equiv; dots), and 0.25 mM ligand (5 equiv; long dashes). The ligands are (A) *N*-meim; (B) 1,4-dib; (C) 1,5-dip, and (D) 1,6-dih.

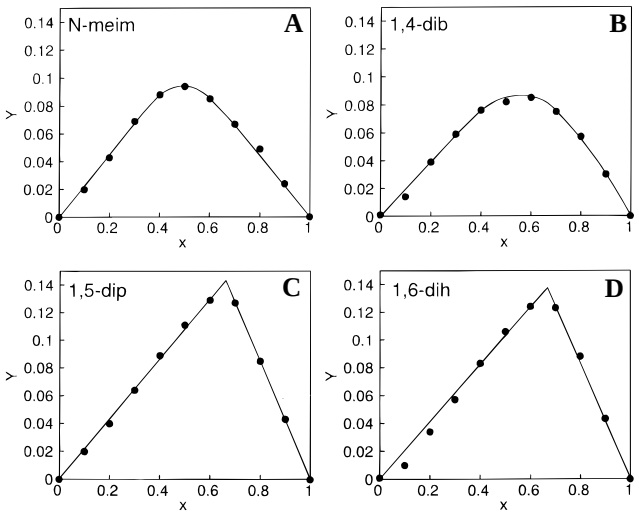

FIGURE 4: Job's plots of *Y* against the mole fraction of His117Gly azurin (×) (see eq 2) with the ligands (A) *N*-meim; (B) 1,4-dib; (C) 1,5-dip; and (D) 1,6-dih. The total concentration of ligand plus protein was 50 μM. The experiments were performed at 298 K in 20 mM Hepes, pH 7.5 (*N*-meim and 1,4-dib) or in 20 mM Mes, pH 6.0 (1,5-dip and 1,6-dih).

bridge between the two imidazole-rings of this ligand is too short to allow for the simultaneous binding of two azurin molecules. To determine more accurately the binding ratio between ligand and azurin a Job's plot was constructed.

Job's Method. Job's plots of *Y* against *x* (the fraction of His117Gly azurin) (see eq 2) are shown in Figure 4. The experiments with *N*-meim and 1,4-dib were performed at pH 7.5 instead of pH 6 because at pH 7.5 the ligands bind stronger to His117Gly azurin and the maxima in the Job's plot are sharper. The maximum of *Y* for the His117Gly azurin and *N*-meim combination occurs at $x_m = 0.5$. This indicates a one to one binding of ligand to azurin (see eq 1). In the case of 1,5-dip and 1,6-dih *Y* has a maximum at $x_m = 0.67$. From this it can be concluded that two azurin molecules bind to one di-*N*-imidazole alkane molecule (see eq 1). In the case of 1,4-dib the maximum of *Y* is not very sharp and has a tendency to move to a position between $x = 0.5$ and 0.67. This indicates that 1,4-dib is able to bind one

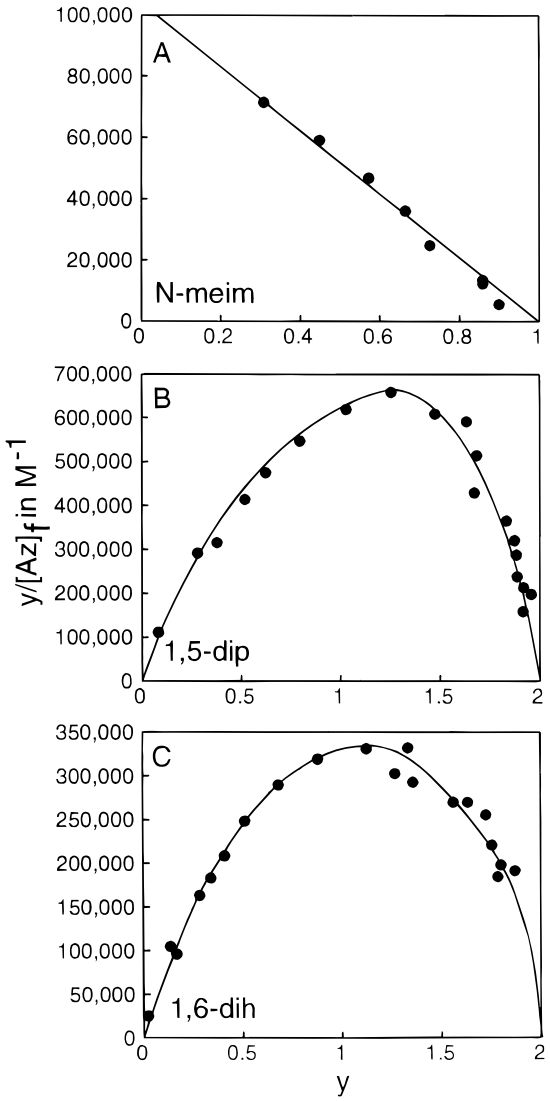

FIGURE 5: Scatchard plots of $y/[Az]_f$ against *y* (see eq 5a) of His117Gly azurin with the ligands (A) *N*-meim; (B) 1,5-dip; and (C) 1,6-dih.

to two azurin molecules, with the species binding one azurin molecule being the more abundant species.

The closest distance in the crystal structure between the metal sites in the azurin dimers is 14.7 Å (Nar et al., 1991a,b). It is found, when using standard bond lengths and angles, that 1,4-dib, 1,5-dip, and 1,6-dih when fully stretched can bridge a distance of 13.9, 15.2, and 16.7 Å, respectively. This is in agreement with the observation that 1,5-dip and 1,6-dih are able to form dimers, whereas 1,4-dib is somewhat too short and only forms dimers in small amounts.

Extinction Coefficients. The plot of the absorbance against the total protein concentration gave straight lines in the cases of 1,5-dip and 1,6-dih (data not shown). This indicates that at the concentrations used in the experiment the His117Gly azurin is saturated with ligand. The values of the extinction coefficients were obtained from the slopes of the plots and are given in Table 1. These coefficients are given per mole of His117Gly azurin. As 1,4-dib gave rise to a mixture of monomers and dimers with His117Gly azurin no unequivocal value of the extinction coefficient could be obtained.

In the case of *N*-meim the plot of the maximum absorbance against the total protein concentration did not result in a straight line. This reflects the presence of an equilibrium between His117Gly azurin and *N*-meim. The extinction

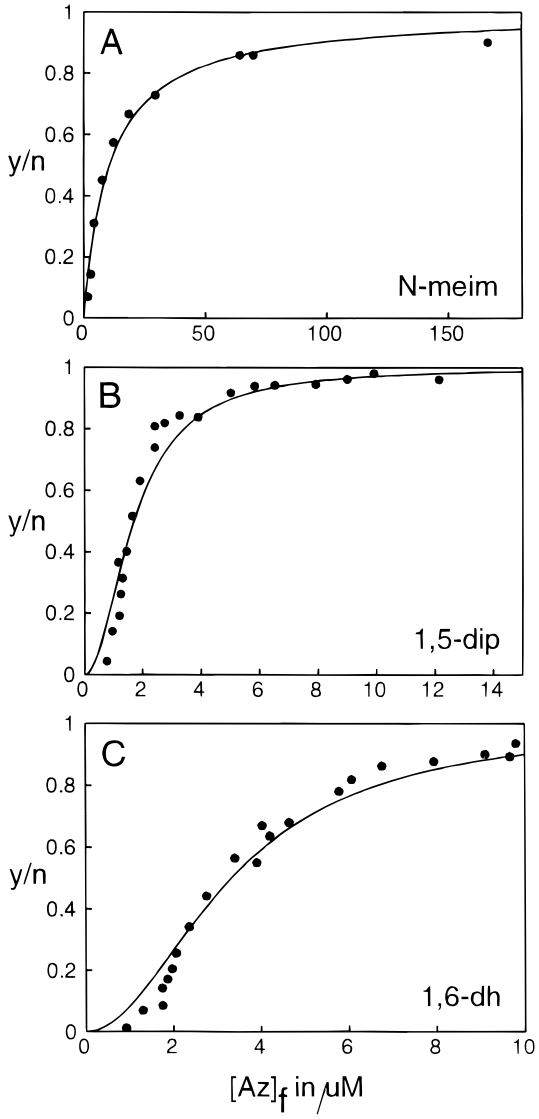

FIGURE 6: Plots of the fractional saturation of ligand (y/n) against free His117Gly azurin ($[Az]_f$) as used for the determination of the binding constant (K_b) (see eq 7) with (A) *N*-meim; (B) 1,5-dip; and (C) 1,6-dih as the ligands. The lines represent the fits of eq 7 with (A) $n = 1$ and $\alpha = 1$; (B and C) $n = 2$ and $\alpha = 2$.

coefficient of the complex of His117Gly with *N*-meim was determined by fitting the data points with eq 8.

$$A_m = [\mathrm{AzL}](\epsilon_b - \epsilon_f) + \epsilon_f[\mathrm{Az}]_t, \quad \text{in which} \qquad (8)$$

$$[\mathrm{AzL}] = {}^1/_2\{\sigma - (\sigma^2 - 4[\mathrm{L}]_t[\mathrm{Az}]_t)^{1/2}\},$$

$$\sigma = [\mathrm{L}]_t + [\mathrm{Az}]_t + 1/K_b, \quad \text{and}$$

$$\epsilon_f = 1.37\ \mathrm{mM}^{-1}\ \mathrm{cm}^{-1}.$$

The value obtained for the extinction coefficient (ϵ_b) is quoted in Table 1.

Scatchard Plots and Hill Coefficients. The Scatchard plots are given in Figure 5. The Scatchard plot of the *N*-meim-His117Gly azurin experiments did result in a straight line (see Figure 5A) with a slope of $-K_b$ of -1.12 (± 0.04) $\times$ 10^5 M^{-1} and an intercept of nK_b of 1.08 (± 0.03) $\times$ 10^5 M^{-1} (see eq 5). This gives $n = 0.96$ (± 0.07), as expected for a ligand with one binding site. When n is fixed to 1 the fit of the data points in Figure 5A gives $K_b = 1.04$ (± 0.03) $\times$ 10^5 M^{-1}. This fit is represented by the line in Figure 5A.

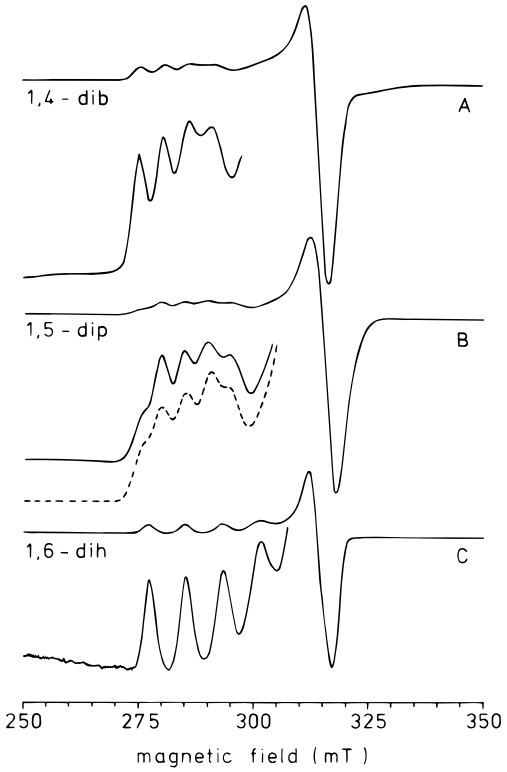

FIGURE 7: X-band EPR spectra of 2 mM samples of His117Gly azurin at 77 K in the presence of (A) 1,4-dib; (B) 1,5-dip; and (C) 1,6-dih in 20 mM Mes buffer, pH 6.2, containing 40% glycerol. The dotted line in (B) represents the sum of the two slightly different species of which the spectra were simulated with parameters given in Table 2. The $g_{//}$, $A_{//}$, and $g_\perp$ values of the other spectra are also given in Table 2.

The Scatchard plots of the 1,5-dip and 1,6-dih complexes with His117Gly azurin gave concave-down curves (see Figure 5B,C). This indicates that there are multiple binding sites with cooperative binding. The values of y are seen to vary between 0 and 2, which is consistent with a protein to ligand ratio of 2 (Jones, 1964).

When y/n is plotted against $[Az]_f$ (see Figure 6) the data can be fitted with eq 7. In the case of *N*-meim this gives values for α and K_b of 1.08 (± 0.09) and 8 (± 2) $\times$ 10^4 M^{-1}, respectively, which are in agreement with the values obtained from the Scatchard plot. In the case of 1,5-dip or 1,6-dih the fits with eq 7 give values for α of 2.9 (± 0.2) and 2.5 (± 0.2), respectively, which exceed the theoretical limit of 2. Apparently, the data are not accurate enough to determine the Hill coefficient α accurately. Reasonable fits, however, can be obtained with α fixed at 2 (as shown in Figure 6B,C). The K_b obtained for the 1,5-dip binding to His117Gly azurin is 3.4 (± 0.3) $\times$ 10^{11} M^{-2} and for 1,6-dih 9.0 (± 0.6) $\times$ 10^{10} M^{-2}.

EPR Spectroscopy. EPR spectra of His117Gly azurin in the presence of 1,4-dib, 1,5-dip, and 1,6-dih are shown in Figure 7.

The EPR spectrum of the His117Gly-1,4-dib complex shows one major species and a species that is present at low concentration (Figure 7A). The major species is ascribed to the complex in which one azurin molecule is bound to the ligand and the minor species derives most likely from a small amount of a complex in which two azurin molecules are bound to the 1,4-dib. The EPR parameters of the major species are given in Table 2.

The His117Gly-1,5-dip dimeric complex exhibits an X-band spectrum with mixed type-1 copper sites (Figure 7B).

Table 2: EPR Parameters of His117Gly Azurin with Exogenous Ligands[a]

ligand	$A_{//}$ (10^{-4} cm^{-1})	$g_{//}$	$g_{\perp}$
His117 (wt)	58	2.260	2.058
1,4-dib[b]	57	2.273	2.058
1,5-dip[c]	55	2.252	2.048
	55	2.280	2.048
1,6-dih[b]	82	2.226	2.053

[a] 20 mM Mes, 40% glycerol, pH 6.2, at 77 K. [b] Estimated error in $A_{//}$, $\pm 2 \times 10^{-4}$ cm^{-1}; in $g_{//}$ and $g_{\perp}$, ± 0.002. [c] The parameters were determined from a simulation in which both species were present in equal amounts. Estimated error in $A_{//}$, $\pm 5 \times 10^{-4}$ cm^{-1}; in $g_{//}$, ± 0.005; and in $g_{\perp}$, ± 0.002.

This spectrum could be simulated by superimposing equal amounts of two slightly different type-1 copper sites of which the parameters are given in Table 2. Considering the tight packing of the two molecules in the His117Gly−1,5-dip dimeric complex, it is conceivable that the exogenous ligand is not able to bind the two proteins in exactly the same manner and as a consequence the two imidazoles are forced into slightly different conformations, thereby creating two slightly different copper centers.

The EPR spectrum of the His117Gly-1,6-dih dimeric complex shows, in contrast to the above case, a single type-1 species (Figure 7C, table 2). Apparently the slightly larger distance between the two imidazole rings of this ligand, leaves each of the two imidazoles sufficient room to adopt an optimal conformation and to form two identical sites.

Cooperativity and Hydrophobic Interactions. The binding of 1,5-dip or 1,6-dih to His117Gly azurin can be described as a two-step binding process with binding constants K_{b1} and K_{b2} (see eqs 6a−d). The binding constant K_b is the product of K_{b1} and K_{b2}. The first step is similar to *N*-meim binding to His117Gly azurin and is expected to have a similar K_b (1×10^5 M^{-1}). Using this value for K_{b1}, K_{b2} can be calculated as 3.4×10^6 and 9.0×10^5 M^{-1} for 1,5-dip and 1,6-dih, respectively. From this it can be seen that there is positive cooperativity in binding of the second azurin molecule, as $K_{b1} < K_{b2}$. The cooperativity arises from the extra gain in free enthalpy (ΔG) upon dimer formation, as given by eq 9 (Cantor & Schimmel, 1980).

$$\Delta G = -RT \ln(K_{b2}/K_{b1}) \tag{9}$$

ΔG amounts to −2.1 kcal/mol for the 1,5-dip and −1.3 kcal/mol for the 1,6-dih case. Assuming that the gain in free enthalpy is caused by the hydrophobic interaction of the two azurin molecules upon the formation of the dimer, an estimate can be obtained of the surface area involved. According to Richards (1977) the gain in free enthalpy upon

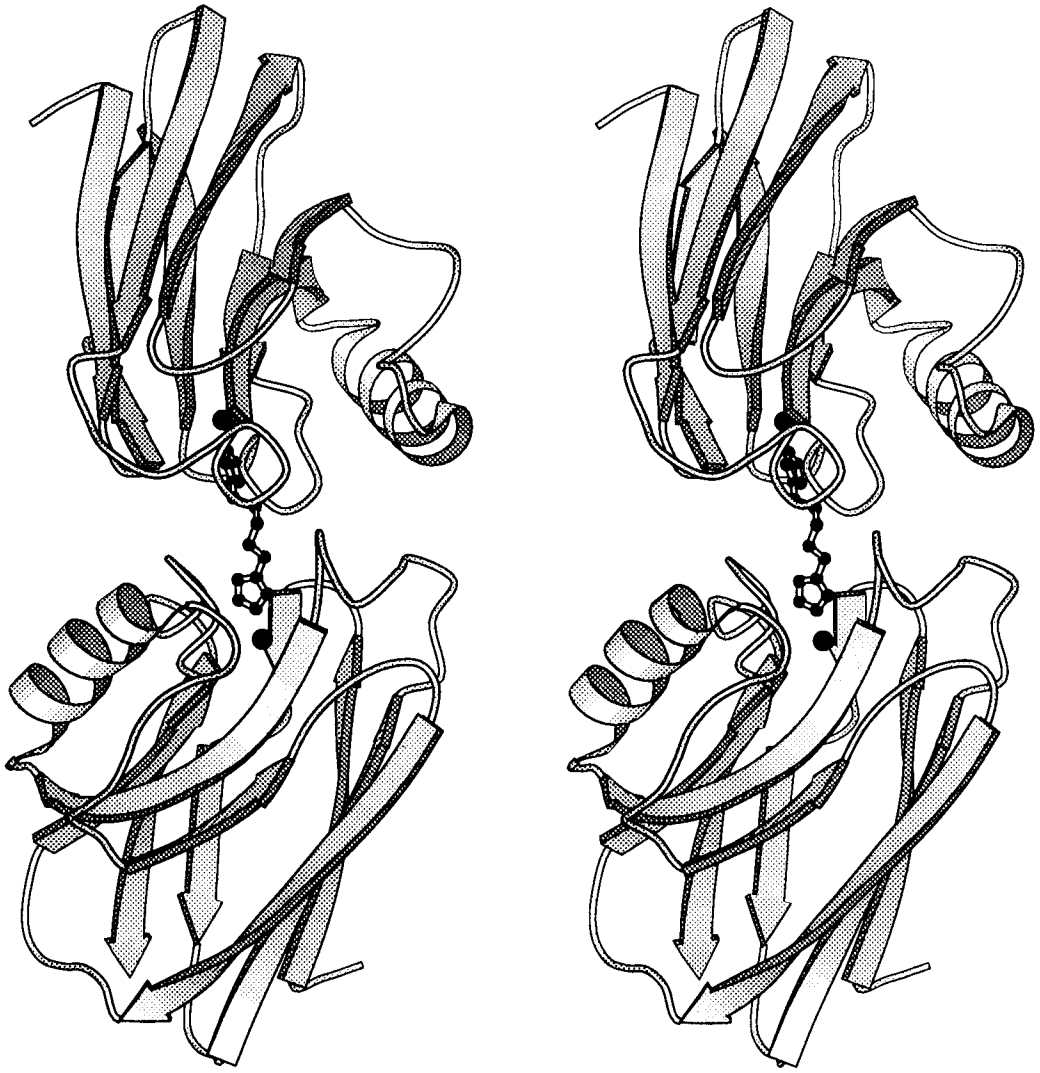

FIGURE 8: Molecular model of the complex between 1,5-dip and His117Gly azurin based on the crystal structure of wt azurin. The imidazole rings of the linker were placed at the positions of the histidine imidazole rings in the crystal structure. The configuration of the $(CH_2)_5$-linker was obtained via energy minimization.

the association of two hydrophobic surfaces is about 20 cal/Å^2. This means that for the 1,5-dip−azurin dimer the contact area amounts to about 105 Å^2 and to about 65Å^2 for the 1,6-dih−azurin dimer. That the hydrophobic interaction is less extensive in the 1,6-dih dimer might be because the dimer is less tightly packed and there is a somewhat less extensive interaction between the hydrophobic patches of the two molecules. The total area of hydrophobic surface in this patch may be roughly estimated as that of a circle with a diameter of 14 Å (distance between Cϵ of Met44 and Cϵ of Met64) and a surface of 154 Å^2. The present data demonstrate that a substantial part of this patch is involved in the dimer formation indeed.

CONCLUSIONS

The results described above have clearly shown that it is possible to create azurin dimers by linking two His117Gly azurins with an 1,ω-di(imidazol-1-yl)alkane linker. The optimum length of the $(CH_2)_m$ bridge between the 2 imidazole-groups is found when *m* equals 5, although the packing of the dimer might be not as tight as in the dimer found in the crystal structure of wt azurin. A model based on this structure, in which with the 1,5-dip linker has been modeled in place, is shown in Figure 8. The data also show that dimer formation is promoted when there is a favorable interaction between surface patches that bind to the opposite ends of the linker.

The present work dealt with homo-dimers and symmetrical bifunctional ligands, but the principle explored here is not limited to this type of construct. Conceptually it can be extended to cases where the linker is not symmetrical and has different end groups as ligands or to cases where different (engineered) proteins are used to form a hetero-dimer. The proteins may have different cavities, created for instance by deleting a particular residue (histidine, methionine) from the coordination sphere of a metal (Cu in blue-copper proteins, Fe in heme-containing proteins) or by removing a complete co-factor [PQQ (pyrroloquinoline quinone), flavin]. The bifunctional linker may contain different ligating groups (imidazole, pyridine, flavin, PQQ) that each preferentially bind to ("recognize") their "own" protein. As shown in this study the dissociation constants for ligand binding can be easily engineered into the micromolar and sub-micromolar range. Applications may range from the study of (macro)-molecular recognition to electron transfer processes along molecular bridges completely buried inside a protein matrix.

ACKNOWLEDGMENT

We thank I. M. M. Schellekens and G. A. van Albada (Leiden) for the synthesis of the bifunctional ligands, N. M. Kostić (Ames, IA) for useful advice on the application of Job's method, Esther Kuyl (Leiden) for assistance in calculating the minimum energy conformation of the 1,5-dip linker in the dimer, and W. R. Hagen (Wageningen) for providing the EPR simulation program.

REFERENCES

Aasa, R., & Vänngård, T. (1975) *J. Magn. Reson. 19*, 308−315.
Barrick, D. (1994) *Biochemistry 33*, 6546−6554.
Barrick, D. (1995) *Curr. Opin. Biotechnol. 6*, 411−418.
Cantor C. R., & Schimmel P. R. (1980) *Biophysical Chemistry, Part III: The Behavior of Biological Macromolecules*, W. H. Freeman and Company, NY.
den Blaauwen, T., & Canters, G. W. (1993) *J. Am. Chem. Soc. 115*, 1121−1129.
den Blaauwen, T., van de Kamp, M., & Canters, G. W. (1991) *J. Am. Chem. Soc. 113*, 5050−5052.
den Blaauwen, T., Hoitink, C. W. G., Canters, G. W., Han, J., Loehr, T. M., & Sanders-Loehr, J. (1993) *Biochemistry 32*, 12455−12464.
Fitzgerald, M. M., Churchill, M. J., McRee, D. E., & Goodin, D. B. (1994) *Biochemistry 33*, 3807−3818.
Hill, A. V. (1910) *J. Physiol. (London) 40*, iv.
Jones, M. M. (1964) *Elementary Coordination Chemistry*, Prentice-Hall, Inc., Englewood Cliffs, NJ.
Lu, Y., Casimiro, D. R., Bren, K. L., Richards, J. H., & Gray, H. B. (1993) *Proc. Natl. Acad. Sci. U.S.A. 90*, 11456−11459.
McRee, D. E., Jensen, G. M. Fitzgerald, M. M., Siegel, H. A., & Goodin, D. B. (1994) *Proc. Natl. Acad. Sci. U.S.A. 91*, 12847−12851.
Nar, H., Messerschmidt, A., Huber, R., van de Kamp, M., & Canters, G. W. (1991a) *J. Mol. Biol. 218*, 427−447.
Nar, H., Messerschmidt, A., Huber, R., van de Kamp, M., & Canters, G. W. (1991b) *J. Mol. Biol. 221*, 765−772.
Pake, G. E., & Estle, T. L. (1973) *The Physical Principles of Electron Paramagnetic Resonance*, 2nd ed., Appendix B, Benjamin, Reading, MA.
Palmer, T. (1991) *Understanding enzymes*, 3rd ed., Ellis Horwood, England.
Richards, F. M. (1977) *Annu. Rev. Biophys. Bioeng. 6*, 151−176.
Roe, A. M. (1963) *J. Chem. Soc.* 2195−2200.
Scatchard, G. (1949) *Ann. N.Y. Acad. Sci. 51*, 660−672.
van Pouderoyen, G., Andrew, C. R., Loehr, T. M., Sanders-Loehr, J., Mazumdar, S., Hill, H. O. A., & Canters, G. W. (1996) *Biochemistry 35*, 1397−1407.
Vidakovic, M., & Germanas, J. P. (1995) *Angew. Chem. 34*, 1622−1624.
Wilks, A., Sun, J., Loehr, T. M., & Oritz de Montellano, P. R. (1995) *J. Am. Chem. Soc. 117*, 2925−2926.

BI960931G